ELSEVIER

Wear 200 (1996) 346–352

WEAR

Shear of confined perfluorinated molecules: Effect of side branching

Yoon-Kyoung Cho, Steve Granick

Dept. of Materials Science and Engineering, University of Illinois, Urbana, IL, 61801, USA

Abstract

To understand the dependence of nanorheology on molecular architecture for perfluorinated molecules, studies were performed using two lubricants commonly used in the magnetic storage industry. Experiments mimicked a single asperity by confining liquids to molecular spacings between atomically smooth mica and applying oscillatory shear forces. The force–distance profiles were compared. Large differences were obtained for the linear shear response. The elastic and dissipative shear moduli of a branched perfluoropolymer (Krytox-AZ) were comparable even at high loads, signifying that the fluid remained fluid-like over experimental frequencies. However, linear perfluoropolymer (Demnum S-20) was easily solidified. The nonlinear responses were also surprising. Previously, we (G. Reiter et al., Science 263 (1994) 1741) reported that the shear-induced transition from an elastic state (at rest) to a dissipative state (during sliding) was discontinuous and hysteric for various hydrocarbon fluids but not for the perfluorinated chain, perfluoroheptaglyme. However, the stick–slip transition was discontinuous, and even more hysteretic for the linear perfluoropolymer (Demnum S-20).

Keywords: Shear; Magnetic storage; Nanorheology; Perfluoropolyether; Confined; Stick-slip

1. Introduction

What are the structure and dynamic properties of a liquid when it is confined to a thickness comparable to the size of the molecules? This question of interfacial rheology and the molecular origin of lubrication has attracted much attention because of the numerous relevant applications and interesting physical phenomena. Examples include stabilization of colloids, polymer adhesives and lubrication [1–9].

Based on the studies with simple liquids [2] and hydrocarbon polymers [5–8], the key experimental findings were the following. The shear moduli are enhanced compared to the bulk, relaxation times are prolonged, and nonlinear responses set in a lower shear rate than in the bulk [8].

What role is played by the chain architecture? There have been studies comparing the force–distance profiles of linear and branched chain hydrocarbon molecules [9]. When simple liquids are confined between solid surfaces, oscillatory force profiles are observed, which means that the liquids tend to form a layered structure extending over several layers [9–19]. This has been investigated experimentally [10,11] and using computer simulations [12–19]. Oscillations persist but in weakened form if the linear chain carries a single methyl branch [9,20,21]. However, a smooth curve with one sole attractive minimum was observed for squalene, a branched chain with six methyl groups [9]. This result suggested that heavy branching can disrupt the extent of layering and thus the oscillatory forces. Then, what are the effects of branching on the shear dynamics? Simple liquids (squalane and the globular silicone tetramer, OMCTS) showed no obvious differences [9,22,23].

In contrast to hydrocarbon molecules, the shear behavior of perfluoropolyethers was reported to be quite different depending on the linear or branched chain structure [24,25]. No oscillatory force distance profile was observed for either branched or linear perfluoropolymers (Fomblin-Y and Fomblin-Z, respectively), presumably because the chain length of these perfluoropolyether samples was much higher than that of simple hydrocarbon liquids.

However, it was reported that whereas the thickness of the linear chains (Fomblin-Z) under large load lessened significantly when shear was applied, this thickness for branched chains (Fomblin-Y) was not affected much by shear [25]. Furthermore, the limiting shear stress of the branched chain was significantly lower than that of the linear chain. In addition, the interesting observation was made that the shear stress of the linear chain was always larger than that of the branched chain under confinement, while the bulk viscosity of the branched chain is about an order of magnitude larger than that of the linear chain [25]. However, a question could be

PII S0043-1648(96)07296-1

Table 1
Physical properties of the samples

	Branched chain (Krytox 143-AZ)[a]	Linear chain (Demnum S-20)[b]
Molecular weight (g mol^{-1})	1850	2500
Density (g cm^{-3})	1.86	1.86
Viscosity, 20 °C (poise)	0.744	0.781
Surface tension, 78.8 F (dyne cm^{-1})	16.0	16.0
Refractive index	1.296	1.290
Molecular structure	CF_3CF_2O–[CF_3–CF–CF_2–O–]$_n$–CF_2–CF_2–CF_3	CF_3CF_2O–[CF_2–CF_2–CF_2–O–]$_n$–CF_2–CF_3

[a] DuPont Performance Products, KRYTOX® Fluorinated Oils. WL-7-8 and WL-7-2 are fractionated samples of Krytox-AZ; in other words, with narrower distribution of molecular weight.
[b] DAIKIN Industries Ltd, High-Performance Fluorocarbon Oil Demnum®.

raised about this comparison since the chain length of the linear sample was almost twice that of the branched one.

According to the study by Homola et al. [25], the presence of side groups in these chains prevents a layered structure from forming and so prevents the film from solidifying. These workers considered that branched molecules are less restricted in their configurations and exhibit more freedom to slide past each other, resulting in lower shear stress [25].

On the other hand, the argument of Pooley and Tabor was that the side groups appear to hinder the translational motion of the polymer chains in relation to each other, resulting in an increase in friction [26].

In this study, we have investigated the dependence of shear rheology on molecular architecture in a confined space with commercially important samples, perfluoropolyethers, which are commonly used as lubricants in magnetic storage devices. First, we measured the static force required to squeeze the films to a given thickness for the branched and linear molecules. Next, we compared the linear viscoelastic behavior of two different chains. Finally, we discussed the shear responses as a function of shear rate.

2. Experimental

2.1. Apparatus

The experimental apparatus [27] and methodology [5] for the static forces and dynamic measurements measured have been discussed previously [5,27]. In brief, the liquid was added by pipette between freshly cleaved atomically smooth muscovite mica surfaces mounted on rigid supports. The film thickness and the flattened contact area were measured by multiple beam interferometry. Sinusoidal shear forces were applied by the piezoelectric bimorph and the response was measured by a second bimorph. The experimental temperature was 27 °C. The sample was kept dry by keeping P_2O_5 inside the surface forces apparatus throughout the experiment.

2.2. Materials

Perfluoropolyether fluids are indispensable to the computer industry as lubricants for magnetic disks because of their many desirable properties, such as low surface tension, high chemical and thermal stability, oxidative resistance and excellent lubricity [27].

Two types of lubricants were investigated. Molecular structures of the samples are summarized in the Table 1. These samples were obtained as a generous donation from Dr Shashi Sharma and Dr Harvey Paige at the U.S. Air Force Wright Patterson Laboratory.

2.3. Data analysis

The same mechanical model which is described in detail in the Ref. [27] was used to analyze the data of the oscillatory shear experiments. Fig. 1 shows the model to separate the response of the sample itself from the compliance in the device. In this model, the mechanical impedance of the piezoelectric device (Z_D) is in parallel with the series combination of the glue (Z_G) and the sample (Z_L). Some portion of the applied force deflects the device and the remainder deflects the serial combination of glue and sample. The measured deflection of the receiver bimorph is equal to the sum of the deflections within the glue and within the sample. The total complex impedance of the sample and glue, $Z=k+i\omega b$, is:

$$1/Z=1/Z_G+1/Z_L \quad (1)$$

where Z_L is the complex impedance of the liquid, $Z_L=k+i\omega b$, and Z_G is that of the glue, $Z_G=k+i\omega b$. Here, k is the spring (elastic) and b is the dashpot (dissipative) coefficient.

It is typical to represent the linear response data in terms of the frequency dependency of effective storage and loss shear moduli, $G_1'(\omega)$ and $G_1''(\omega)$, respectively, where ω is

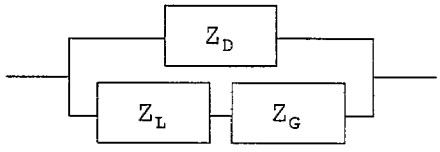

Fig. 1. Mechanical model used to analyze the data. The impedance of the piezoelectric device (Z_D) is in parallel with the series combination of the glue (Z_G) and the sample (Z_L). Each component is the series combination of the spring constant (k) and dashpot coefficient (b).

the angular frequency of sinusoidal oscillation [29]. The dynamic moduli are related to the spring constant and dash part coefficient of the liquid by the geometry factor:

$$G_1' = (h/A)K_L \quad (2)$$

$$G_1'' = (h/A)\omega b_L \quad (3)$$

where A is the contact area, h is the film thickness. The storage modulus, G_1', is the elastic component of the shear stress which is in-phase with the deformation. The loss modulus, G_1'', is the dissipative component which is in phase with the shear rate, $\dot{\gamma}_{eff}$ the rate of deformation of the film. Although these equations only take account of the first harmonic term, these are used for the strain dependency of the dynamic moduli even in the nonlinear region simply because it is easy to calculate and much larger than the higher order terms.

Even though the definition of viscosity is subtle for the inhomogeneous systems because the local viscosity would vary with distance across a thin liquid film, the effective viscosity, η_{eff}, is usually used as a quantity that is correlated to the resistance of the fluid to flow. Effective viscosity is defined as the viscous stress divided by shear rate and it is related with loss moduli with following equation:

$$\eta_{eff} = \tau_{vis}/\dot{\gamma}_{eff} = G_1''/\omega \quad (4)$$

where $\dot{\gamma}_{eff}$ is the effective shear rate which is defined as the maximum shear amplitude divided by the film thickness and τ_{vis} is the viscous stress term. The detail of the calibration and analysis are described elsewhere [5,22,27].

3. Results and discussion

3.1. Static forces

Fig. 2 shows the force–distance profiles of the branched chain molecule (Krytox-AZ) and the linear chain (Demnum S-20). Monotonic repulsive forces were observed for both of the samples. The thickness of Krytox-AZ under load ≈ 5 MPa was 30 Å whereas Demnum S-20 showed the much larger thickness of 50 Å at the same level. The equilibration time between the points was 45 min for Krytox-AZ and 10 min for Demnum S-20; sufficient in both cases to reach steady state.

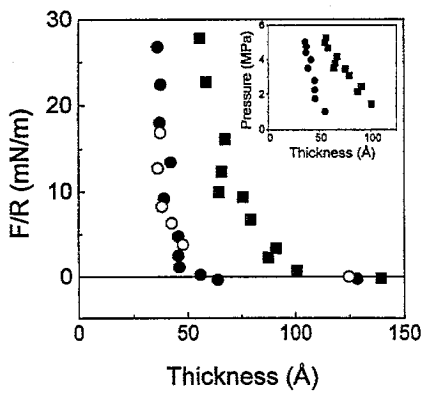

Fig. 2. The static force, F, normalized by the mean radius of curvature, R, of the crossed cylindrical surfaces plotted against the liquid film thickness. Inset: pressure–thickness relation for Demnum-S20 and Krytox-AZ. Squares are Demnum-S20 and circles are Krytox-AZ. Filled circles denote measurements during compression and open circles denote measurements made during increase of film thickness.

It is important to note that a higher force was needed to squeeze the branched chain than the linear chain. It was easily squeezed up to about 50 Å and then a strong repulsive force was measured for the branched chain. Thickness change was small with further compression. On the other hand, for the linear chain, the repulsive force began to be measured at about 100 Å and the film thickness was easily decreased with compression. In addition, the contact area increase of the branched chain was small when large load was applied, whereas the linear chain showed a large increase of contact area with compression. Therefore, the pressure increased rapidly with compression for the branched chain while it was slow for the linear chain as shown in the inset of Fig. 2.

The static force measurement were done with small shear amplitude (< 1 Å) and at low frequency (1.3 Hz). The linear chain was solidified as compressed and the elastic moduli were dominant from about 100 Å. However, the branched chain was not solidified (no damping was observed) even under strong confinement and the moduli were still negligible. It is understandable that the solidified film of the linear chain deformed the surface more and thus increased the contact area during the compression, while the non-solidified branched chain was easily squeezed out and thus didn't deform the surface so much.

Under high load, however, the branched sample formed relatively thin films. This may reflect the fact that the branched chain is believed to be stiffer and to have a longer persistence length (locally, a more rodlike structure) because of the high energy for chain rotation [25]. Therefore these chains might be more apt to align parallel to the surface. Note also that compared to the Krytox-AZ, Demnum-S20 had longer chain contour length (both had almost the same average total molecular weight). The Demnum-S20 would as a result be more intertwined with other chains, also tending to give a thicker film under a given normal load.

Homola and coworkers showed previously that the thickness of linear Fomblin, under large load, was larger than of branched chains [25]. However, these differences of molecular architecture were not clearly separated because whereas the linear (Fomblin-Z) sample was of relatively high molecular weight, the molecular weight of the branched counterpart (Fomblin-Y) was much lower.

Based on the above observations, one can say that branched chains appear to make better lubricants in the sense that the thickness change is less sensitive to the pressure while remaining fluid-like than linear chains, and at the same time form thinner films. In terms of the application to hard disk devices, the ability of Krytox to form thinner films may be desirable because lubricant films of thickness larger than 20–

50 Å of lubricant are easily spun off by centrifugal forces [28].

3.2. Linear viscoelastic responses

When shear deformations are small enough to give a linear response, stress is directly proportional to strain and the measurement is believed to probe the unperturbed structure of the sample [5]. The experiments described below were performed at different frequencies but always at shear amplitude so small that it did not disturb the sample structure.

Fig. 3 shows the storage and loss shear moduli of Demnum S-20 plotted against angular frequency on the log–log scales. The linear sample was very easily solidified and displayed shear moduli larger than the other samples discussed below. The storage moduli exceeded the loss moduli and showed negligible frequency dependence. This is the typical result for solidified liquids under strong confinement [2,8].

In contrast, the data of Krytox-AZ in Fig. 4 are quite unusual and surprising because the storage and the loss moduli were still comparable in magnitude even under high load, which means that the films were not solidified. At these loads

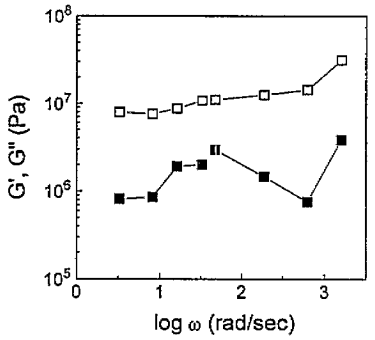

Fig. 3. Frequency dependence of the storage modulus (open symbols) and the loss modulus (closed symbols) of Demnum S-20 under very low load. The film thickness was 97 Å. Note that the storage moduli were larger than the loss moduli and flat through the range of frequency studied. The moduli of these linear chains were an order of magnitude larger than those of Krytox-AZ. Results were not changed qualitatively when the load was increased. Scatter in the data for the low modulus (filled symbols) is because these data were an order of magnitude less than the storage modulus.

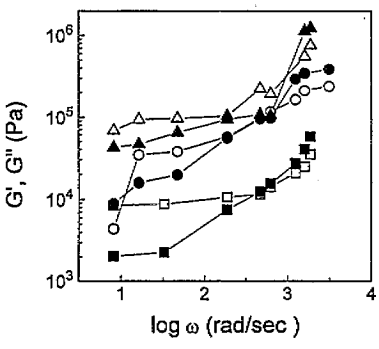

Fig. 4. Frequency dependence of the storage modulus (open symbols) and the loss modulus (closed symbols) of the branched chain (Krytox-AZ). The film thickness was 20 Å but the load was varied: 3.5 MPa (squares), 4.0 MPa (circles), and 4.4 MPa (triangles). Note that the storage moduli and the loss moduli are comparable in magnitude.

(corresponding to normal pressures of 3.5 to 4.4 MPa), the film thickness remained constant at 20 Å. While the magnitude of the shear moduli increased with increasing normal load, their ratio remained approximately unity regardless of the load. This has never been observed from our previous studies of hydrocarbon liquids. For the hydrocarbon liquids, when the load was high, the storage moduli were always bigger than the loss moduli and constant throughout the range of frequency studied [2,5–8].

The data suggest that Krytox-AZ might be a good lubricant because it was not solidified even at the very largest loads. In other words, the branched chain has a lower friction coefficient than the linear one. But why is it so? Is it because of the fluorinated chemistry or the branched structure?

3.2.1. Fractionated samples

It was difficult, with a polydisperse sample, to separate the effects of molecular architecture and molecular weight. We now discuss measurements on the two fractionated samples, the low (WL-7-2) and high (WL-7-8) molecular weight fractions of Krytox identified in Section 2.2. These fractions had been separated by supercritical extraction from a polydisperse sample of Krytox-AZ.

Fig. 5 compares the storage and loss moduli of the low and high molecular weight fractions, and of the parent sample of polydisperse Krytox-AZ, plotted versus the sinusoidal shear frequency. These had been measured at low load where the samples begin to display the repulsive forces shown in Fig. 2; the moduli were even larger when the load was higher. At these low loads, the moduli were larger in magnitude, the higher the molecular weight. However at the same time, for every sample, the storage and loss moduli were always comparable in magnitude, showing a relative lack of solidification regardless of the molecular weight. Therefore, one can say that the cause was indeed branched molecular architecture.

For the fractionated sample of lowest molecular weight, Fig. 6A shows the storage and loss moduli at fixed film thickness of 39 Å plotted against strain amplitude at 1.3 Hz and

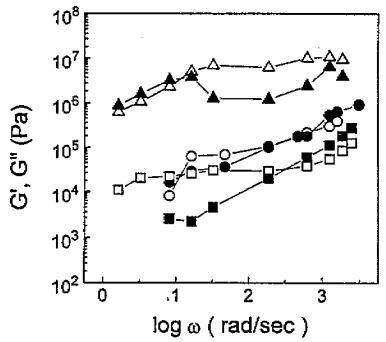

Fig. 5. Frequency dependence of the storage modulus (open symbols) and the loss modulus (closed symbols) of Krytox samples of varying molecular weight. Squares: fractionated sample of low molecular weight fractions (Krytox WL-7-2, thickness 18 Å). Circles: polydisperse Krytox-AZ (thickness 20 Å). Triangles: fractionated sample of high molecular weight (Krytox WL-7-8, thickness 43 Å). The fraction of higher molecular weight showed solidification when the load was raised.

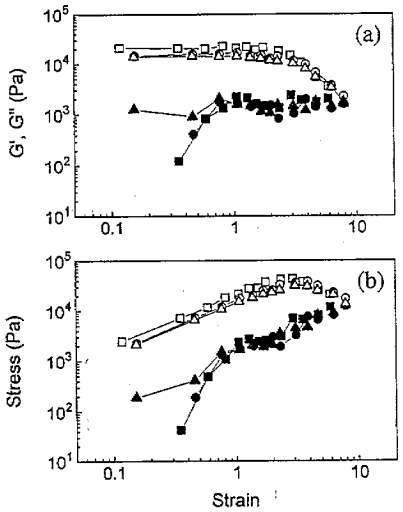

Fig. 6. Strain dependence of the storage modulus (open symbols) and the loss modulus (closed symbols) of the low molecular weight fraction of Krytox-AZ (Krytox WL-7-2) at constant thickness of 20 Å and frequency 1.3 Hz. As the load was varied, the contact area was estimated using Hertz theory. In the bottom panel, the elastic stress (open symbols) and the viscous stress (closed symbols) stress are plotted against the strain. The load was ~0 (squares), 3.6 MPa (circles), and 11.0 MPa (triangles).

loads of 3.6, 8.7, and 11.0 MPa. The storage moduli were constant up to about the strain of 2 and subsequently decreased with increasing strain. The loss moduli were almost constant through the range of strain studied. It is useful to recall that strain is defined as shear displacement divided by film thickness. It is truly remarkable that this sample could withstand such a high strain.

It is also informative to consider these same data expressed in terms of stresses (force per unit area) rather than moduli. The elastic and dissipative stresses are plotted against strain in Fig. 6B. The shear stresses actually decreased with increasing load. This is because the contact area (measured directly in these experiments by multiple beam interferometry) increased more rapidly than the increase of friction stress. Compared to the sharp and discontinuous stick–slip transition observed, at large load, for a branched hydrocarbon [22], this sample displayed a rather smooth and continuous change.

Fig. 7A shows the strain dependence of the shear moduli for the high molecular weight fraction of Krytox-AZ at the frequency of 1.3 Hz. The elastic and dissipative stresses are also plotted versus strain in Fig. 7B. Fig. 8A and 8B compare results at the frequency of 100 Hz. These measurements have been done at small load but the same thickness (43 Å) as at large load. Three features of these data are particularly interesting. First, for this sample the moduli were larger in magnitude than for the sample of lower molecular weight. Second, the strain at the stick–slip transition was smaller. Finally, the linear behavior held up to higher strain at 100 Hz than 1.3 Hz.

At high load, only solid-like behavior was observed over the range of strain amplitude studied. This was probably due to the difficulty of distorting this strongly confined structure at high frequency.

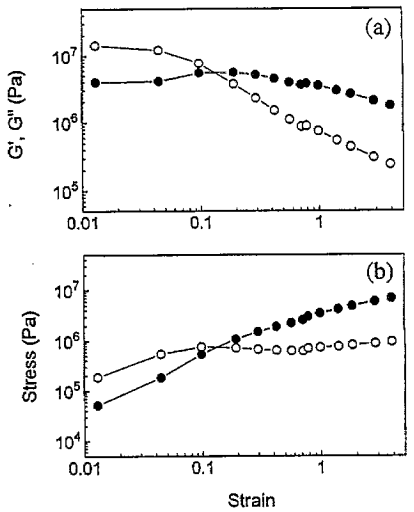

Fig. 7. Strain dependence of the storage modulus (open symbols) and the loss modulus (closed symbols) of the high molecular weight fraction of Krytox-AZ (Krytox WL-7-8) at very low load (thickness 43 Å) and frequency 1.3 Hz. In the bottom panel, the elastic stress (open symbols) and viscous stress (closed symbols) are plotted against the strain.

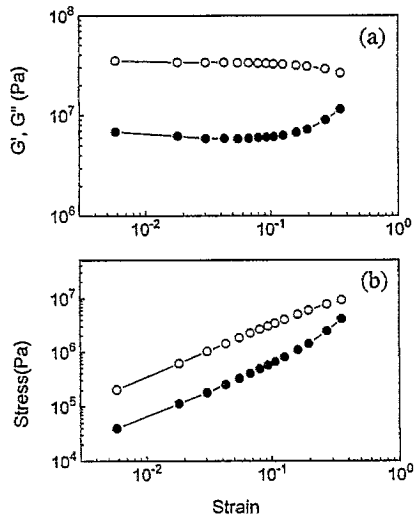

Fig. 8. Strain dependence of the storage modulus (open symbols) and the loss modulus (closed symbols) of the high molecular weight fraction of Krytox-AZ (Krytox WL-7-8) at very low load (thickness 43 Å) and frequency 100 Hz. In the bottom panel, the elastic stress (open symbols) and viscous (closed symbols) are plotted against the strain. Note that compared to Fig. 6 (lower frequency), linear behavior held to higher strain.

3.3. Stick to slip transition

As described above, Demnum S-20 displayed abrupt stick–slip transitions. In an earlier study, we reported that the shear induced transition from elastic to dissipative state was discontinuous for hydrocarbon fluids but not for a fluorinated fluid, perfluoroheptaglyme [22,23]. The present experiments suggest however that this was an unusual case; a discontinuous stick to slip transition was observed for Demnum S-20, very similar to the results with a branched hydrocarbon [22].

An example is shown in Fig. 9. The sample showed solid-like behavior up to a critical strain. The data were measured

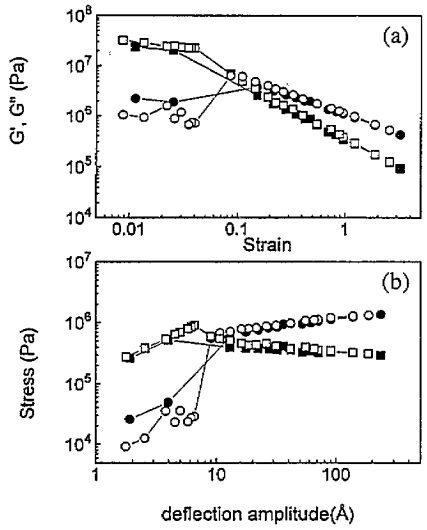

Fig. 9. The storage modulus (squares) and loss modulus (circles) of Demnum S-20 (a linear perfluorinated chain) at very low load (thickness 72 Å) and frequency 1.3 Hz. In the bottom panel, the responding elastic stress (squares) and viscous stress (circles) are plotted against deflection amplitude on log–log scales. The closed symbols represent data taken with increasing strain and the open symbols data taken with decreasing strain, thus demonstrating reversibility.

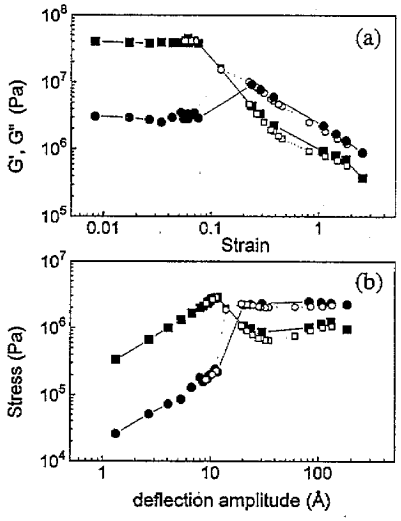

Fig. 10. The storage modulus (squares) and loss modulus (circles) of Demnum S-20 at very low load (thickness 72 Å) and frequency 100 Hz. Bottom panel: see caption to Fig. 9.

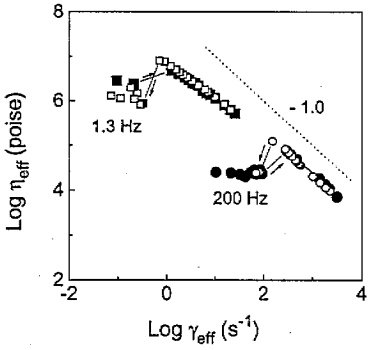

Fig. 11. Effective viscosity plotted against effective shear rate on log–log scales. Data from two experiments are shown. Squares are 1.3 Hz, circles 200 Hz. The closed symbols represent data taken with increasing strain and the open symbols data taken with decreasing strain.

at low load at thickness 72 Å and at 1.3 Hz. The top panel shows the strain dependence of the storage and loss moduli and the bottom panel shows the corresponding viscous and elastic stresses as a function of deflection amplitude. The storage moduli were largest up to a critical strain, above which the loss moduli were largest and both showed shear thinning. In the former case the response was predominantly elastic; in the latter it was predominantly dissipative. When we decreased the shear amplitude to check reversibility, we observed remarkable hysteresis. In particular, we could reach lower strains, and still retain kinetic friction, than when shear amplitude was raised. Interestingly, we could reach higher stress when we decreased the shear amplitude. However, this state was unstable. In particular, small vibrations induced a return transition, from the dissipative back to the elastic state.

Similar results were obtained at higher frequency (200 Hz) as shown in Fig. 10, except that the transition in this case occurred at higher strain.

Some readers may be more familiar with the notion of dynamic viscosity, η_{eff}, than of shear modulus. They are related, however: dynamic viscosity is the loss modulus divided by excitation frequency. Fig. 11 shows this effective viscosity plotted against the shear rate at two frequencies, 1.3 and 200 Hz. In the stick regime, the effective viscosity was constant. After the stick–slip transition from the elastic to the dissipative state, shear thinning was observed. The effective viscosity decreased as a power law in the shear rate, $\eta_{eff} \propto \dot{\gamma}_{eff}^{-\alpha}$, with slope $2/3 \leq \alpha \leq 1$. Interestingly, the data of the two experiments at two different frequencies but high shear rate extrapolate to fall on the same line.

This power-law decrease is also observed for the shear thinning of confined hydrocarbon fluids [2,4,6]. Various theoretical models predict this result [19,30–33]. At higher shear rates, as the limiting shear stress of the lubricant is approached, the power law of shear thinning approached the slope of -1 as expected. The new result in the present data is to show that these perfluoropolymers displayed liquid-like shear thinning at high shear rate. It is surprising to see static friction at low shear rate followed the liquid-like non-Newtonian response when the shear rate was high. The power law which characterized the shear thinning was observed for hydrocarbon samples that exhibit no static friction.

4. Conclusion

In summary, we have studied the dependence of shear rheology on molecular architecture for confined perfluoropolyether fluids. First, a distinctive difference was observed from the static force measurement. Although linear and branched chains both showed repulsive force profiles, the branched chain (Krytox-AZ) was much harder to compress

than the linear chain (Demnum-S20) and displayed a smaller film thickness when the load was high. Moreover, the contact area of the branched chain film did not change much with compression while the linear chains were easily squeezed out as the contact area was increased.

We assume the linear chain formed thicker films than the branched chains, at a given load, because its contour length is larger than that of the branched chain. Moreover, one can understand that the surface was deformed more and thus the contact area increased more rapidly for the linear chain due to the solidification. On the other hand, the branched chain was not solidified under strong confinement, which possibly suggests that the branched chain may have more space and easy to slip over each other.

Secondly, interesting differences were observed in the linear shear viscoelastic response. Whereas the linear chains were easily solidified by load, even at the highest load studied the branched chain (Krytox-AZ) was not found to solidify. Control experiments with fractionated samples of different molecular weight confirmed this result, though the sample of higher molecular weight showed higher absolute values of shear moduli.

It is interesting to note the previous study with Demnum-8k whose molecular weight is 8000 [34]. This sample was less prone to solidify.

Finally, as the shear rate was increased far beyond the point of linear response, the branched chain (Krytox-AZ) showed a continuous and smooth transition to a kinetic dissipative state. In contrast, the linear chain showed a discontinuous and abrupt stick to slip transition.

These experimental observations suggest that this branched chain might possess superior lubrication properties. We speculate that the role of the $-CF_3$ side groups might be twofold. On the one hand, they may impede the formation of layered structure (that is, density waves normal to the surface) and in this way impede solidification. On the other hand, they appeared to somehow provide more space for adjoining molecules to slip over one another. This was reflected in the fact that, at even at the highest shear rates studied, the viscous stress continued to increase with shear rate and the limiting shear stress response was not yet attained. But it is interesting to note that studies of confined squalane show that $-CH_3$ side groups on a hydrocarbon lubricant [23] does not have this effect. Thus, the effect of chain branching can be very different for perfluorinated than for hydrocarbon chains.

Acknowledgements

We are indebted to Dr. Shashi Sharma and Dr. Harvey Paige at the U.S. Air Force Wright Patterson Laboratory for the generous gift of samples. We thank Ali Dhinojwala, Lenore L. Cai and A. Levent Demirel for discussions. This work was supported by grants from the Exxon Research & Engineering Corp. and the U.S. Air Force (AFOSR-URI-F49620-93-1-02-41).

References

[1] J.V. Alsten and S. Granick, *Phys. Rev. Lett., 61* (1988) 2570.
[2] H. Hu, G.A. Carson and S. Granick, *Phys. Rev. Lett., 66* (1991) 2758.
[3] H. Hu and S. Granick, *Science, 258* (1992) 1339.
[4] S. Granick, *Science, 253* (1991) 1374.
[5] S. Granick and H. Hu, *Langmuir, 10* (1994) 3857.
[6] S. Granick, H. Hu and G.A. Carson, *Langmuir, 10* (1994) 3867.
[7] J. Peanasky, L.L. Cai, C.R. Kessel and S. Granick, *Langmuir, 10* (1994) 3867.
[8] L.L. Cai, J. Peanasky and S. Granick, *Trends Polym. Sci., 2* (1996) 47.
[9] S. Granick, A.L. Demirel, L.L. Cai and J. Peanasky, *Israel J. Chem., 35* (1995) 75.
[10] R.G. Horn and J.N. Israelachvili, *J. Chem. Phys., 75* (1981) 1400.
[11] J.N. Israelachvili, *Intermolecular and Surface Forces*, Academic Press, San Diego, 2nd edn., 1992.
[12] P.B. Balbuena, D. Berry and K.E. Gubbins, *J. Phys. Chem., 97* (1993) 937.
[13] K. Walley, K.S. Schweizer, J. Peanasky, L.L. Cai and S. Granick, *J. Phys. Chem., 100* (1994) 3361.
[14] C.L. Jr. Rhykerd, M. Schoen, D.J. Diestler and J.H. Cushman, *Nature, 330* (1987) 461.
[15] P.A. Thompson and M.O. Robbins, *Phys. Rev. A., 41* (1990) 6830.
[16] M. Schoen, C.L. Rhykerd, D.J. Diestler and J.H. Cushman, *Science, 245* (1989) 1223.
[17] P.A. Thompson and M.O. Robbins, *Science, 250* (1990) 792.
[18] M.W. Ribarsky and U.J. Landman, *J. Chem. Phys., 97* (1992) 1937.
[19] P.A. Thompson, G.S. Grest and M.O. Robbins, *Phys. Rev. Lett., 68* (1992) 3448.
[20] J.N. Israelachvili, S.J. Kott, M.L. Gee and T.A. Witten, *Macromolecules, 22* (1989) 4247.
[21] M.L. Gee and J.N. Israelachvili, *J. Chem. Soc. Faraday Trans., 86* (1990) 4049.
[22] G. Reiter, A.L. Demirel and S. Granick, *Science, 263* (1994) 1741.
[23] G. Reiter, A.L. Demirel, J. Peanasky, L.L. Cai and S. Granick, *J. Chem. Phys., 101* (1994) 2606.
[24] J.P. Monfort and G. Hadziioannou, *J. Chem. Phys., 88* (1988) 7187.
[25] A.M. Homola, H.V. Nguyen and G. Hadziioannou, *J. Chem. Phys., 94* (1991) 2346.
[26] C.M. Pooley and D. Tabor, *Proc. R. Soc., A329* (1972) 251.
[27] J. Peachey, J.V. Alsten and S. Granick, *Rev. Sci. Instrum., 62* (1991) 463.
[28] A.M. Homola, C.M. Mate and G.B. Street, *MRS Bull., 45* (1990) 45.
[29] J.D. Ferry, *Viscoelastic Properties of Polymers*, Wiley, New York, 3rd edn., 1980.
[30] M. Urbakh, L. Daikhin and J. Klafter, *Europhys. Lett., 32* (1995) 125.
[31] M. Urbakh, L. Daikhin and J. Klafter, *J. Chem. Phys., 103* (1995) 10707.
[32] E. Manias, J. Bitsanis, G. Hadziioannou and G.T. Brinke, Macromolecules, in press.
[33] E. Manias, *Ph.D. Thesis*, State University of Groningen, The Netherlands, 1995.
[34] J. Peanasky, *Ph.D. Thesis*, University of Illinois, 1995.